Outline

follows the structure of the report

- Introduction
- Mesh-based Modeling of Cuts
- Finite Element Simulation for Virtual Cutting
- Numerical Solvers
- Meshfree Methods
- Summary & Application Study
- Discussion & Conclusion

Major Articles Surveyed in this Report

Reference	Geometry	Deformation	Solver	Scenario	Remark
Bielser et al. [BMG99, BG00, BGTG04]	Tet., refinement	Mass-spring	Explicit/Semi-implicit	Interactive	Basic tet. refinement
Cotin et al. [CDA00]	Tet., deletion	Tensor-mass	Explicit	Interactive	Hybrid elastic model
Mor & Kanade [MK00]	Tet., refinement	FEM	Explicit	Interactive	Progressive cutting
Nienhuys et al. [NFvdS00, NFvdS01]	Tet., boundary splitting/snapping	FEM	Static (CG solver)	Interactive	FEM with a CG solver
Bruyns et al. [BSM*02]	Tet., refinement	Mass-spring	Explicit	Interactive	An early survey
Steinemann et al. [SHGS06]	Tet., refinement + snapping	Mass-spring	Explicit	Interactive (Fig. 13 a)	Hybrid cutting
Chentanez et al. [CAR*09]	Tet., refinement	FEM	Implicit (CG solver)	Interactive (Fig. 13 d)	Needle insertion
Courtecuisse et al. [CJA*10, CAK*14]	Tet., deletion/refinement	FEM	Implicit (CG solver)	Interactive (Fig. 13 c,e)	Surgery applications
Molino et al. [MBF04]	Tet., duplication	FEM	Mixed explicit/implicit	Offline	Basic virtual node algorithm
Sifakis et al. [SDF07]	Tet., duplication	FEM		Offline (Fig. 12 a)	Arbitrary cutting
Jeřábková & Kuhlen [JK09]	Tet.	XFEM	Implicit (CG solver)	Interactive	Introduction of XFEM
Turkiyyah et al. [TKAN09]	Tri.	2D-XFEM	Static (direct solver)	Interactive	XFEM with a direct solver
Kaufmann et al. [KMB*09]	Tri./Quad.	2D-XFEM	Semi-implicit	Offline (Fig. 12 c)	Enrichment textures
Frisken-Gibson [FG99]	Hex., deletion	ChainMail	Local relaxation	Interactive	Linked volume
Jeřábková et al. [JBB*10]	Hex., deletion	CFEM		Interactive	CFEM
Dick et al. [DGW11a]	Hex., refinement	FEM	Implicit (multigrid)	Offline/Interactive (Fig. 12 d)	Linked octree, multigrid solver
Seiler et al. [SSSH11]	Hex., refinement	FEM	Implicit	Interactive	Octree, surface embedding
Wu et al. [WDW11, WBWD12, WDW13]	Hex., refinement	CFEM	Implicit (multigrid)	Interactive (Fig. 13 b, f)	Collision detection for CFEM
Wicke et al. [WBG07]	Poly., splitting	PFEM	Implicit	Offline (Fig. 12 b)	Basic polyhedral FEM
Martin et al. [MKB*08]	Poly., splitting	PFEM	Semi-implicit	Offline	Harmonic basis functions
Pauly et al. [PKA*05]	Particles, transparency	Meshfree	Explicit	Offline	Fracture animation
Steinemann et al. [SOG06]	Particles, diffraction	Meshfree		Offline/Interactive (Fig. 12 e)	Splitting fronts propagation
Pietroni et al. [PGCS09]	Particles, visibility	Meshfree		Interactive	Splitting cubes algorithm

Publication Year – Method Plot

- Trends: from mass-spring systems to finite element methods
- Tetrahedral elements are consistently improved
- Hexahedral elements are recently advocated

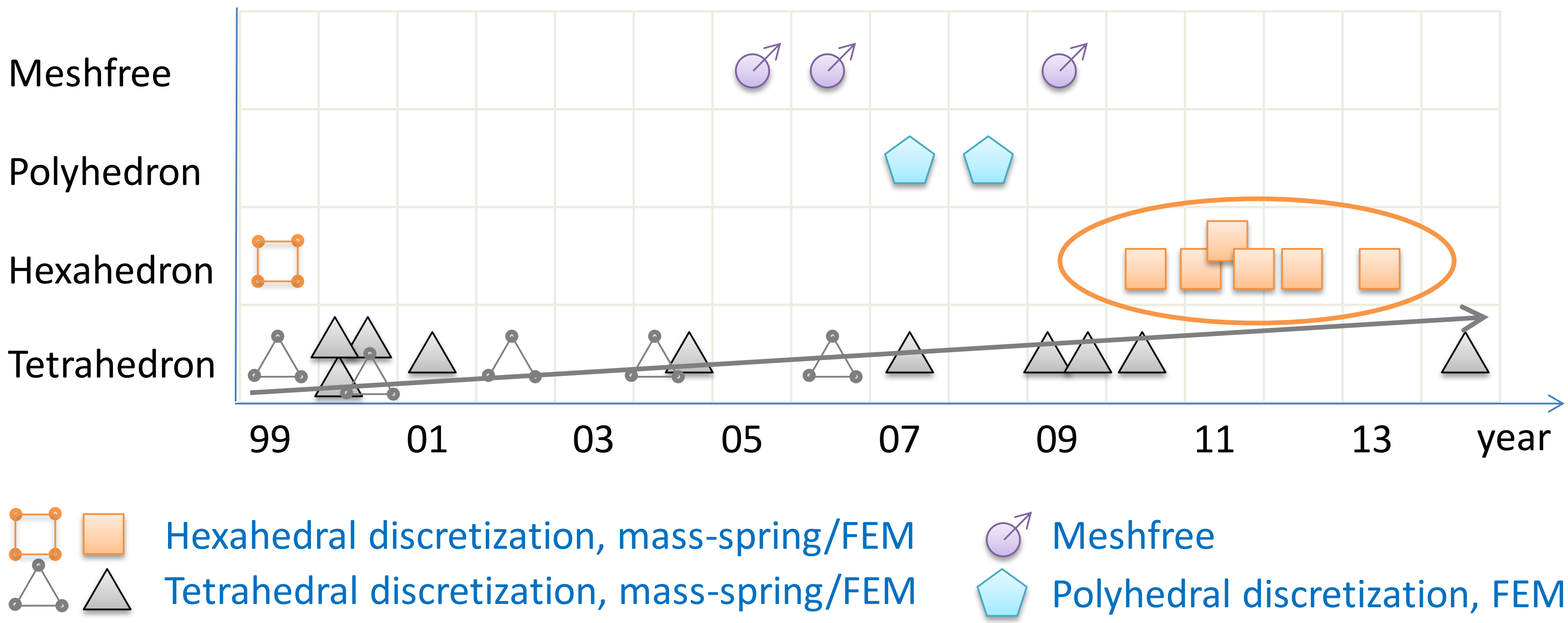

Overview

- Geometrically accurate separation can be supported by all spatial discretizations

Polyhedral FEM
[Wicke et al 2007]

Hexahedral FEM
[Dick et al 2011]

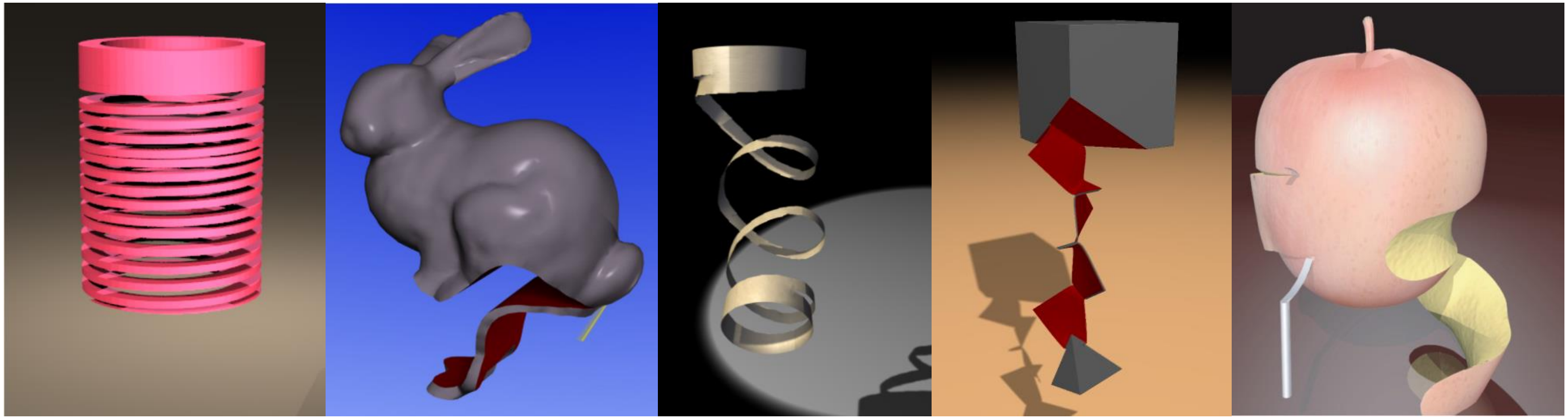

Tetrahedral,
virtual node algorithm
[Sifakis et al 2007]

Quadrilateral,
extended FEM
[Kaufmann et al. 2009]

Meshfree
[Steinemann et al 2011]

Overview

- Tetrahedral discretizations are widely employed in virtual cutting in surgery simulators

Reference	Geometry	Deformation	Solver	Scenario	Remark
Bielser et al. [BMG99, BG00, BGTG04]	Tet., refinement	Mass-spring	Explicit/Semi-implicit	Interactive	Basic tet. refinement
Cotin et al. [CDA00]	Tet., deletion	Tensor-mass	Explicit	Interactive	Hybrid elastic model
Mor & Kanade [MK00]	Tet., refinement	FEM	Explicit	Interactive	Progressive cutting
Nienhuys et al. [NFvdS00, NFvdS01]	Tet., boundary splitting/snapping	FEM	Static (CG solver)	Interactive	FEM with a CG solver
Bruyns et al. [BSM*02]	Tet., refinement	Mass-spring	Explicit	Interactive	An early survey
Steinemann et al. [SHGS06]	Tet., refinement + snapping	Mass-spring	Explicit	Interactive (Fig. 13 a)	Hybrid cutting
Chentanez et al. [CAR*09]	Tet., refinement	FEM	Implicit (CG solver)	Interactive (Fig. 13 d)	Needle insertion
Courtecuisse et al. [CJA*10, CAK*14]	Tet., deletion/refinement	FEM	Implicit (CG solver)	Interactive (Fig. 13 c,e)	Surgery applications
Molino et al. [MBF04]	Tet., duplication	FEM	Mixed explicit/implicit	Offline	Basic virtual node algorithm
Sifakis et al. [SDF07]	Tet., duplication	FEM		Offline (Fig. 12 a)	Arbitrary cutting
Jeřábková & Kuhlen [JK09]	Tet.	XFEM	Implicit (CG solver)	Interactive	Introduction of XFEM
Turkiyyah et al. [TKAN09]	Tri.	2D-XFEM	Static (direct solver)	Interactive	XFEM with a direct solver
Kaufmann et al. [KMB*09]	Tri./Quad.	2D-XFEM	Semi-implicit	Offline (Fig. 12 c)	Enrichment textures
Frisken-Gibson [FG99]	Hex., deletion	ChainMail	Local relaxation	Interactive	Linked volume
Jeřábková et al. [JBB*10]	Hex., deletion	CFEM		Interactive	CFEM
Dick et al. [DGW11a]	Hex., refinement	FEM	Implicit (multigrid)	Offline/Interactive (Fig. 12 d)	Linked octree, multigrid solver
Seiler et al. [SSSH11]	Hex., refinement	FEM	Implicit	Interactive	Octree, surface embedding
Wu et al. [WDW11, WBWD12, WDW13]	Hex., refinement	CFEM	Implicit (multigrid)	Interactive (Fig. 13 b, f)	Collision detection for CFEM
Wicke et al. [WBG07]	Poly., splitting	PFEM	Implicit	Offline (Fig. 12 b)	Basic polyhedral FEM
Martin et al. [MKB*08]	Poly., splitting	PFEM	Semi-implicit	Offline	Harmonic basis functions
Pauly et al. [PKA*05]	Particles, transparency	Meshfree	Explicit	Offline	Fracture animation
Steinemann et al. [SOG06]	Particles, diffraction	Meshfree		Offline/Interactive (Fig. 12 e)	Splitting fronts propagation
Pietroni et al. [PGCS09]	Particles, visibility	Meshfree		Interactive	Splitting cubes algorithm

Overview

- Tetrahedral discretizations are widely employed in virtual cutting in surgery simulators

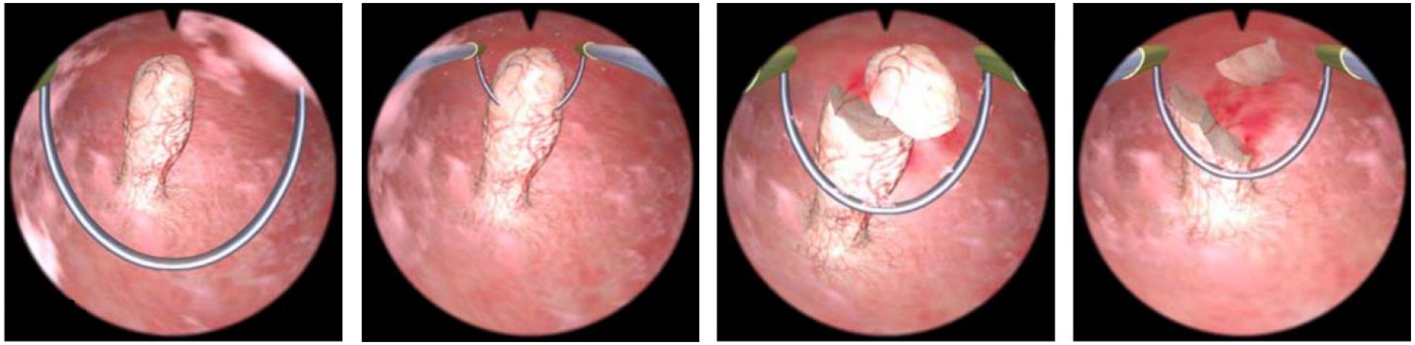

Ablating a polyp in a hysteroscopy simulator [Steinemann et al 2006]

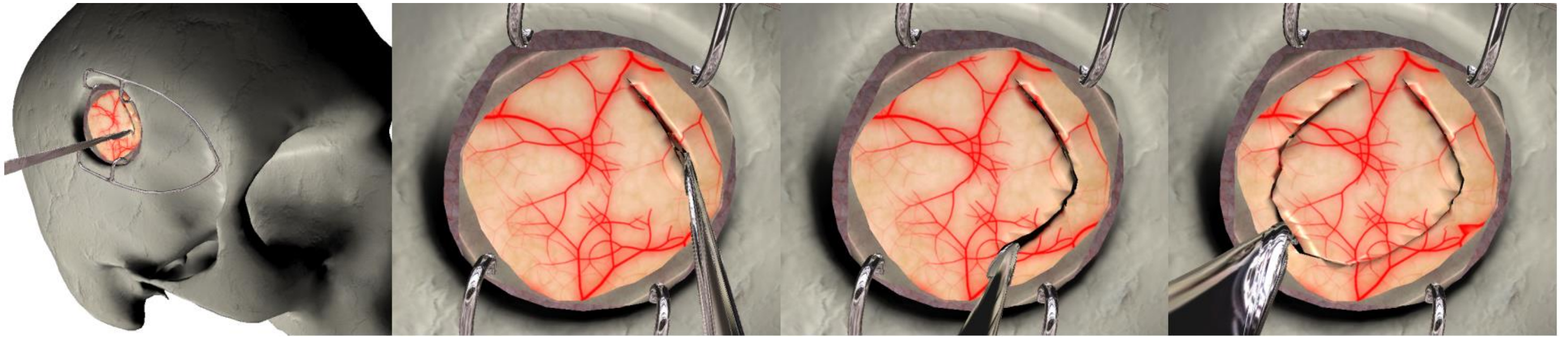

Simulation of a brain tumor resection [Courtecuisse et al 2014]

Overview

- Tetrahedral discretizations are widely employed in virtual cutting in surgery simulators

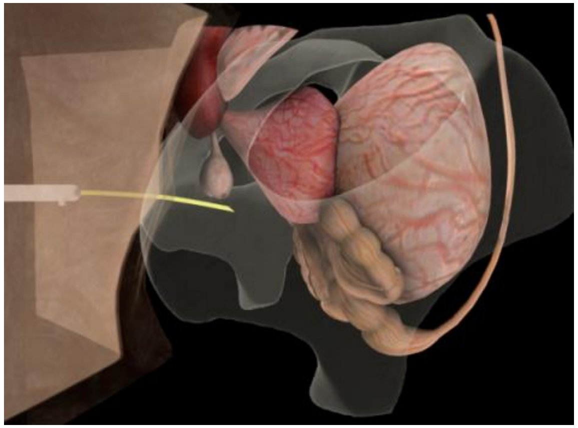

Needle insertion in a prostate brachytherapy simulator

[Chentanez et al 2009]

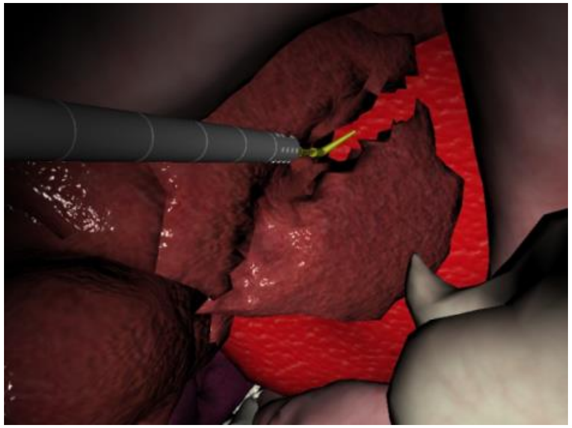

Real-time simulation of laparoscopic hepatectomy

[Courtecuisse et al 2010]

Overview

- Hexahedral discretizations are recently demonstrated to provide a good balance between speed and accuracy

Reference	Geometry	Deformation	Solver	Scenario	Remark
Bielser et al. [BMG99, BG00, BGTG04]	Tet., refinement	Mass-spring	Explicit/Semi-implicit	Interactive	Basic tet. refinement
Cotin et al. [CDA00]	Tet., deletion	Tensor-mass	Explicit	Interactive	Hybrid elastic model
Mor & Kanade [MK00]	Tet., refinement	FEM	Explicit	Interactive	Progressive cutting
Nienhuys et al. [NFvdS00, NFvdS01]	Tet., boundary splitting/snapping	FEM	Static (CG solver)	Interactive	FEM with a CG solver
Bruyns et al. [BSM*02]	Tet., refinement	Mass-spring	Explicit	Interactive	An early survey
Steinemann et al. [SHGS06]	Tet., refinement + snapping	Mass-spring	Explicit	Interactive (Fig. 13 a)	Hybrid cutting
Chentanez et al. [CAR*09]	Tet., refinement	FEM	Implicit (CG solver)	Interactive (Fig. 13 d)	Needle insertion
Courtecuisse et al. [CJA*10, CAK*14]	Tet., deletion/refinement	FEM	Implicit (CG solver)	Interactive (Fig. 13 c,e)	Surgery applications
Molino et al. [MBF04]	Tet., duplication	FEM	Mixed explicit/implicit	Offline	Basic virtual node algorithm
Sifakis et al. [SDF07]	Tet., duplication	FEM		Offline (Fig. 12 a)	Arbitrary cutting
Jeřábková & Kuhlen [JK09]	Tet.	XFEM	Implicit (CG solver)	Interactive	Introduction of XFEM
Turkiyyah et al. [TKAN09]	Tri.	2D-XFEM	Static (direct solver)	Interactive	XFEM with a direct solver
Kaufmann et al. [KMB*09]	Tri./Quad.	2D-XFEM	Semi-implicit	Offline (Fig. 12 c)	Enrichment textures
Frisken-Gibson [FG99]	Hex., deletion	ChainMail	Local relaxation	Interactive	Linked volume
Jeřábková et al. [JBB*10]	Hex., deletion	CFEM		Interactive	CFEM
Dick et al. [DGW11a]	Hex., refinement	FEM	Implicit (multigrid)	Offline/Interactive (Fig. 12 d)	Linked octree, multigrid solver
Seiler et al. [SSSH11]	Hex., refinement	FEM	Implicit	Interactive	Octree, surface embedding
Wu et al. [WDW11, WBWD12, WDW13]	Hex., refinement	CFEM	Implicit (multigrid)	Interactive (Fig. 13 b, f)	Collision detection for CFEM
Wicke et al. [WBG07]	Poly., splitting	PFEM	Implicit	Offline (Fig. 12 b)	Basic polyhedral FEM
Martin et al. [MKB*08]	Poly., splitting	PFEM	Semi-implicit	Offline	Harmonic basis functions
Pauly et al. [PKA*05]	Particles, transparency	Meshfree	Explicit	Offline	Fracture animation
Steinemann et al. [SOG06]	Particles, diffraction	Meshfree		Offline/Interactive (Fig. 12 e)	Splitting fronts propagation
Pietroni et al. [PGCS09]	Particles, visibility	Meshfree		Interactive	Splitting cubes algorithm

Overview

- Hexahedral discretizations are recently demonstrated to provide a good balance between speed and accuracy

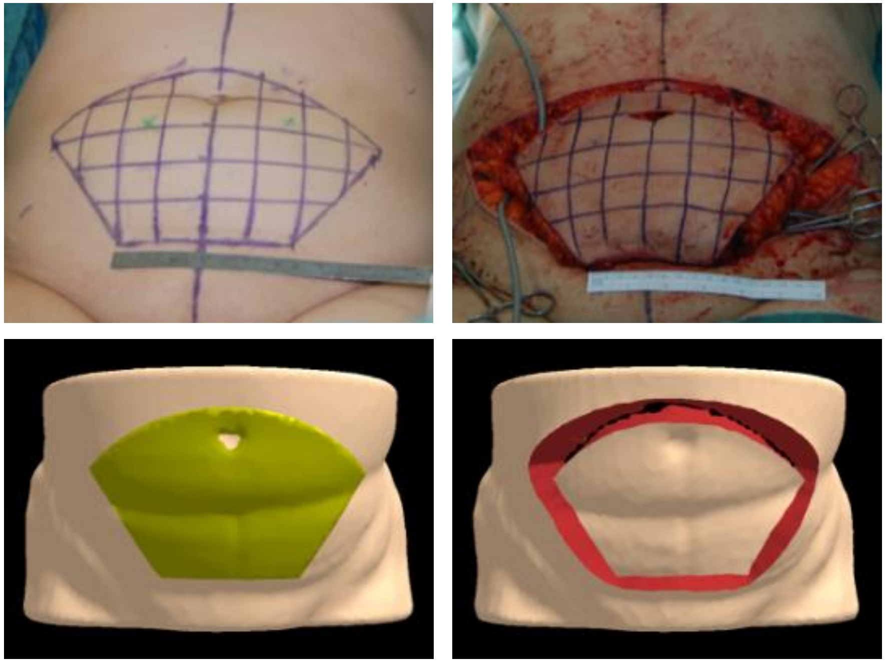

Virtual soft tissue cutting
and shrinkage simulation

[Wu et al 2012]

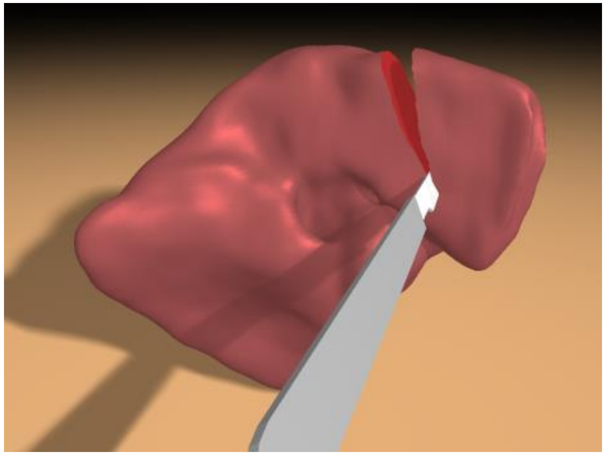

Haptic-enabled virtual cutting
of high-resolution soft tissues

[Wu et al 2014]

Purposes of Application Study

- Provide an estimation of the performance of virtual cutting
- Identify performance bottlenecks in the simulation loop
- Exam accuracy and performance of adaptive methods

- Not an evaluation of all techniques
- But a detailed analysis of our implementations of three variants of hexahedral finite elements

Experimental Setup

- Linear elastic material, corotational strain formulation

- Standard desktop PC
  - Intel Xeon X5560 processor (a single core was used)
  - 8 GB main memory
- Haptic device
  - Sensable Phantom Premium 1.5

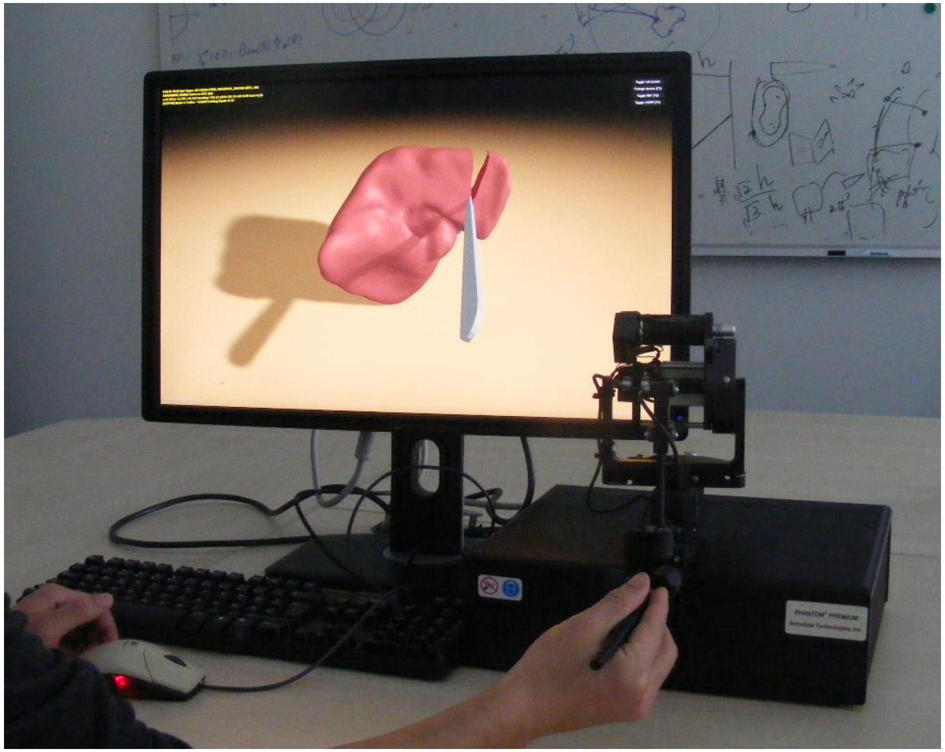

Three Variants

- Basis
  - Geometry modeling: hexahedral elements
  - Surface reconstruction: dual contouring
  - Numerical solver: multigrid solver
- Variants
  - FEs on a uniform hexahedral grid
  - FEs on an adaptive octree grid
  - Composite FEs on an adaptive octree grid

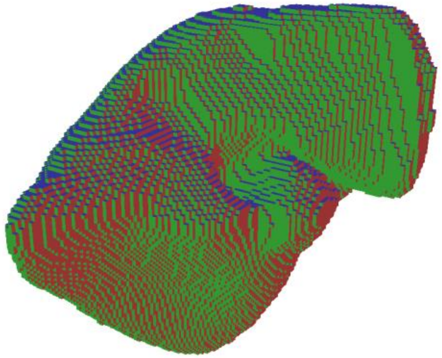

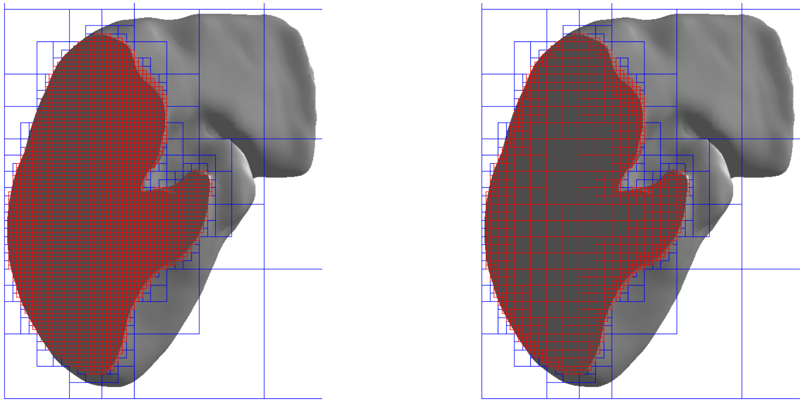

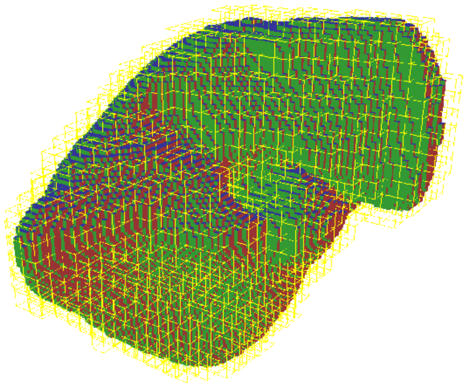

Model Information of Three Variants

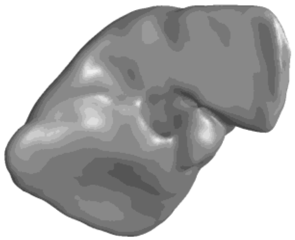

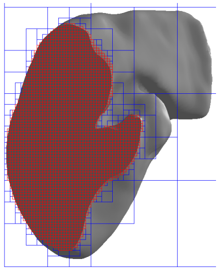

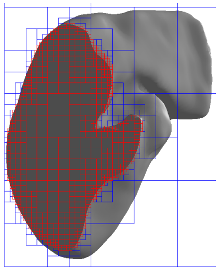

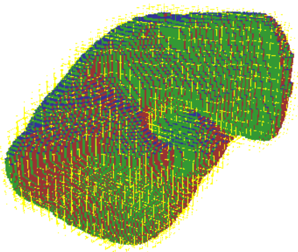

	Uniform	Adaptive	Composite (2 levels)
Coarse resolution		21×21×25	21×21×25
Refined resolution	82×83×100	82×83×100	82×83×100
# Cells (initial)	173 843	40 080	3 439
# DOFs (initial)	566 493	129 162	13 557
# Cells (added due to cut)	0	1 596	39
# DOFs (added due to cut)	2 037	6 438	318

Simulation Results

- Adaptive octree deformation resembles the uniform approach
- Composite simulation results in a slightly stiffer deformation

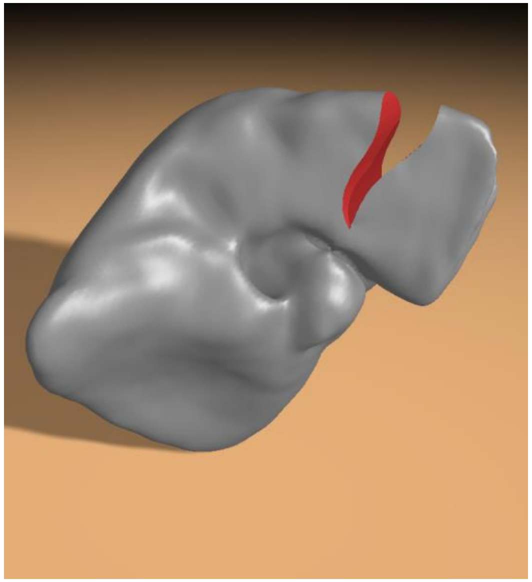

FEs on
a uniform hexahedral grid

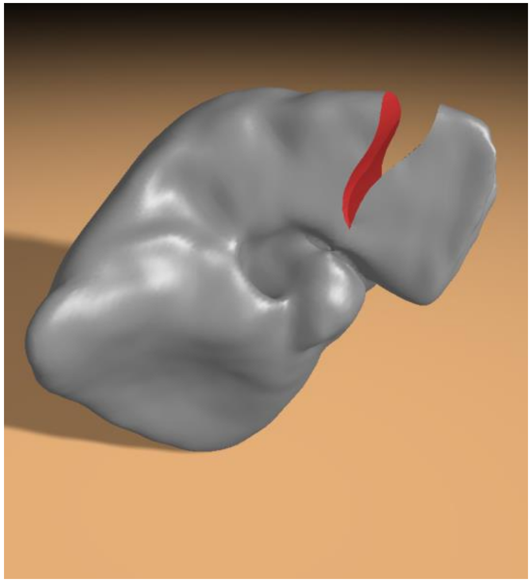

FEs on
an adaptive octree grid

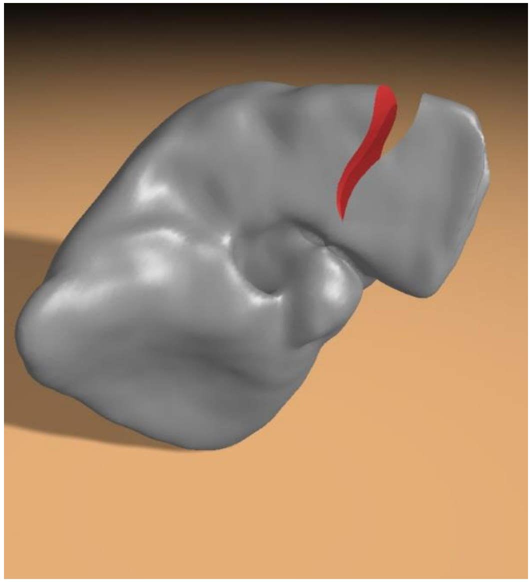

Composite FEs on
an adaptive octree grid

Timings

- Accurate cutting simulation can be performed at 2 seconds per frame, on a uniform 82×83×100 grid

	Uniform
Coarse resolution	
Refined resolution	$\boxed{82\times83\times100}$
# DOFs (initial)	566 493
Octree subdivision (t_1)	0
Surface meshing (t_2)	1.26
FE matrices (t_3)	29.57
Multigrid hierarchy (t_4)	40.34
Solver (t_5)	2 033.09
Simulation per cut ($\sum_{i=1}^{5} t_i$)	$\boxed{2\,104.26}$

Timing
in milliseconds

Timings

- Numerical solver is the bottleneck in cutting simulation

	Uniform
Coarse resolution	
Refined resolution	82×83×100
# DOFs (initial)	566 493
Octree subdivision (t_1)	0
Surface meshing (t_2)	1.26
FE matrices (t_3)	29.57
Multigrid hierarchy (t_4)	40.34
Solver (t_5)	2 033.09
Simulation per cut ($\sum_{i=1}^{5} t_i$)	2 104.26

Timing
in milliseconds

Timings

- Adaptive octree improves the performance by a factor of 3.5

	Uniform	Adaptive
Coarse resolution		21×21×25
Refined resolution	82×83×100	82×83×100
# DOFs (initial)	566 493	129 162
Octree subdivision (t_1)	0	13.29
Surface meshing (t_2)	1.26	1.26
FE matrices (t_3)	29.57	7.05
Multigrid hierarchy (t_4)	40.34	10.09
Solver (t_5)	2 033.09	581.66
Simulation per cut ($\sum_{i=1}^{5} t_i$)	2 104.26	613.35

Timing
in milliseconds

Timings

- Interactive cutting (12 fps) is possible on a 21×21×25 composite simulation grid

	Uniform	Adaptive	Composite (2 levels)
Coarse resolution		21×21×25	$\boxed{21\times21\times25}$
Refined resolution	82×83×100	82×83×100	82×83×100
# DOFs (initial)	566 493	129 162	13 557
Octree subdivision (t_1)	0	13.29	13.39
Surface meshing (t_2)	1.26	1.26	1.24
FE matrices (t_3)	29.57	7.05	20.99
Multigrid hierarchy (t_4)	40.34	10.09	2.06
Solver (t_5)	2 033.09	581.66	40.61
Simulation per cut ($\sum_{i=1}^{5} t_i$)	2 104.26	613.35	$\boxed{78.29}$

Timing
in milliseconds

Timings

- Solver, FE matrices, octree subdivision affect the performance in the composite approach

	Uniform	Adaptive	Composite (2 levels)
Coarse resolution		21×21×25	21×21×25
Refined resolution	82×83×100	82×83×100	82×83×100
# DOFs (initial)	566 493	129 162	13 557
Octree subdivision (t_1)	0	13.29	13.39
Surface meshing (t_2)	1.26	1.26	1.24
FE matrices (t_3)	29.57	7.05	20.99
Multigrid hierarchy (t_4)	40.34	10.09	2.06
Solver (t_5)	2 033.09	581.66	40.61
Simulation per cut ($\sum_{i=1}^{5} t_i$)	2 104.26	613.35	78.29

Timing
in milliseconds

Timings

- Time of surface meshing is negligible

	Uniform	Adaptive	Composite (2 levels)
Coarse resolution		21×21×25	21×21×25
Refined resolution	82×83×100	82×83×100	82×83×100
# DOFs (initial)	566 493	129 162	13 557
Octree subdivision (t_1)	0	13.29	13.39
Surface meshing (t_2)	1.26	1.26	1.24
FE matrices (t_3)	29.57	7.05	20.99
Multigrid hierarchy (t_4)	40.34	10.09	2.06
Solver (t_5)	2 033.09	581.66	40.61
Simulation per cut ($\sum_{i=1}^{5} t_i$)	2 104.26	613.35	78.29

Timing
in milliseconds